# UC Riverside
## 2018 Publications

**Title**
ECEF position accuracy and reliability in the presence of differential correction latency

**Permalink**
https://escholarship.org/uc/item/4t498587

**Authors**
Rahman, F.
Aghapour, E.
Farrell, J.A.

**Publication Date**
2018

Peer reviewed

# ECEF Position Accuracy and Reliability in the Presence of Differential Correction Latency

Farzana Rahman, Elahe Aghapour and Jay A. Farrell

Department of Electrical and Computer Engineering,

University of California, Riverside, 92521.

{frimi, eaghapour, farrell}@ee.ucr.edu

*Abstract*—Many applications, including connected and autonomous vehicles, would benefit from navigation technologies reliably achieving sub-meter position accuracy. Differentially corrected single frequency Global Navigation Satellite Systems (GNSS) are a suitable low cost solution. Differential corrections delivered to a roving vehicle on a nationwide scale will be subject to latency between their time-of-applicability and their time-of-reception at the vehicle. The main contribution of this article is a study of the effect of this communication latency on the position estimation accuracy. An additional contribution of this article is a comparison, using identical measurements and corrections, of the position estimation accuracy as a function of the estimation algorithm. Special attention is given to the accommodation of non-common mode errors. The article specifically focuses on the probability of achieving sub-meter accuracy with latencies up to 600 seconds.

## I. Introduction

A new generation of applications (e.g., autonomous vehicles, connected vehicles, and driver's assistance applications [1], [2]) are placing much stricter accuracy and reliability specifications on navigation systems than was required for the previous generation of personal navigation devices. Over the last several decades, Global Navigation Satellite Systems (GNSS) has become dominant for personal navigation and standard GNSS accuracy [3], [4] of about 10 m is typically sufficient.

The FHWA, state DOTs, and auto manufacturers are investigating connected and autonomous highway vehicle applications which will benefit real-time, ECEF position estimates accurate to sub-meter levels at 95% probability. Pilot projects are ongoing in at least three locations [5]–[7]. The objectives are to improve roadway network safety, while decreasing the emissions impact, through connected vehicle technologies.

Commonly cited position accuracy levels derived from differential GNSS (DGNSS) are 1-3 meters [8]. The lower end of this range makes GNSS systems infeasible for such applications, if this accuracy is not sufficiently reliable and if it is not sensitive to communication latencies.

Navigation systems [9] achieving these accuracy and reliability specifications have not yet been demonstrated. For a national scale of implementation, topics of interest include: communication physical layers, network design for real-time applications, position error sensitivity to communication latency, and estimation algorithms to achieve the accuracy specification.

This article will study positioning error as a function of communication latency and discuss modeling and estimation algorithm choices as they affect positioning algorithm performance. Section III presents notation and background related to the measurement and error models for our problem statement. Section IV presents a differential correction latency compensation approach. Section V discusses use of the Doppler measurement especially as it relates to improving the ability to discriminate the multipath errors. Section VI presents experimental results that show the improvement in positioning performance that is achieved by latency compensation; multipath state augmentation; and use of Doppler to enhance the degree-of-observability.

## II. Related Work

Vehicle positioning by DGNSS is a well researched area [10]–[16]. The literature presents extensive position estimation theory, algorithm, and experimental results that illustrate alternative modeling choices and their impact on performance and reliability [17]–[19].

One important aspect of DGNSS positioning is the sensitivity of position error to baseline separation and communication latency. References [20]–[23] present methods to construct networked differential correction services, ultimately leading to nationwide differential correction service (e.g., WAAS, EGNOS). Various pre-2001 papers [13], [14], [24]–[27] characterize the degradation of positioning accuracy as a function of latency in the era of selective availability (SA). Due to the design of SA, the correction error and hence the position error grew rapidly over tens of seconds. Methods to compensate for communication latency over low bandwidth channels for real-time applications is discussed in [13], [14]. The literature currently lacks studies of real-time positioning performance versus correction latency in the post-SA data.

Multipath error is the dominant error source in differentially corrected GNSS measurements. The literature provides a few methods to address the issue. In [28], the author introduces a narrow correlator based tracking loop system that provided a 20 to 50 percent reduction in multipath error effects for the L1 pseudorange measurement. In [29], [30], a multipath error modeling is addressed using dual frequency carrier phase measurements in a GNSS antenna array system. Choke ring antennae [31] are another option, but are not practical for

inexpensive on vehicle applications. Lastly, many implementations augment one (or more) multipath states per satellite to the state vector. Use of Doppler measurement improves positioning performance by estimating the velocity [32]–[35]. A less well understood benefit of the Doppler measurement is that it enhances the degree-of-observability of the multipath states. This topic will be discussed in Section V.

## III. Problem Statement

This section introduces notation for the GNSS measurement and error models, discusses the necessity of DGNSS technique and delineates various issues that must be addressed to achieve sub-meter positioning accuracy. For additional information on GNSS, see [9], [17], [18].

The GNSS receiver provides three different types of measurements: pseudorange, Doppler and carrier phase measurements. At present, low-cost consumer applications do not incorporate carrier phase. This article focuses on pseudorange and Doppler.

The pseudorange measurement model is

$$\rho_r^s \doteq R(P_r, P^s) + ct_r - ct^s + I^s + T^s + M_r^s + \eta_r^s \qquad (1)$$

where

$$R(P_r, P^s) = |P_r - P^s|. \qquad (2)$$

The symbol $R(P_r, P^s)$ represents the range from receiver $r$ to satellite $s$, $ct_r$ is receiver clock bias, $ct^s$ is satellite clock bias, $I^s$ is ionospheric error, $T^s$ is tropospheric error, $M_r^s$ is multipath error, and $\eta_r^s$ is receiver pseudorange noise.

The Doppler $D_r^s$ measurement model is

$$\lambda D_r^s \doteq (h^s)^T(v_r - v^s) + cb_r - cb^s + \varepsilon_r^s \qquad (3)$$

where

$$h^s = \frac{P_r - P^s}{|P_r - P^s|} \qquad (4)$$

is the line-of-sight vector from receiver $r$ to satellite $s$, $v_r$ and $v^s$ are the receiver and satellite velocity vectors, $cb_r$ and $cb^s$ are the receiver and satellite clock drift rates, and $\varepsilon_r^s$ is Doppler measurement noise.

The pseudorange measurement has 7 different types of errors. They can be classified into two categories: common-mode and noncommon-mode. Common-mode errors (ephemeris, satellite clock bias, ionosphere, troposphere) are common to all receivers in nearby vicinity and can be mitigated with the use of DGNSS corrections. Noncommon-mode errors (receiver clock bias, multipath, receiver noise) are different for each receiver. This paper discusses methods to manage both types of errors to achieve sub-meter positioning accuracy.

## IV. DGNSS Correction Approach

DGNSS is the typical approach to remove common-mode errors from pseudorange measurements [12], [17]. DGNSS can be implemented on global or local scales. For a global approach, network of GNSS receivers measure the GNSS signals, estimate information to broadcast to users such that each user can reconstruct a local correction [21], [22]. Ultimately, DGNSS on a commercial scale will implement such network DGNSS methods. In such approaches, for real-time commercial applications on vehicles, correction convergence times and robustness to communication latency will be critical.

A primary goal of this paper is to study the sensitivity of positioning accuracy to communication latency. For the purpose of this study, it is sufficient to utilize local corrections. For the local approach used in this paper, which is a variant of the RTCM standard [10], the correction convergence time is zero, once the base station message is received.

The local base station algorithm used for the results herein is designed to be robust to latency and base station multipath error. The local base station position $P_b$ is known.

At time $t$ the base station algorithm computes

$$\tilde{c}(t) = \rho_b^s(t) - R(P_b, \hat{P}^s(t)) + c\hat{t}_b(t) - c\hat{t}^s(t) \qquad (5)$$

where $R(P_b, \hat{P}^s)$ is computed using eqn. 2, $\rho_b^s$ is the base pseudorange measurement, $\hat{P}^s$ and $\hat{t}^s$ are the satellite position and clock bias computed from ephemeris data, and $c\hat{t}_b(t)$ is an estimate of the base receiver clock bias. Typically, the magnitude of $\tilde{c}(t)$ is less than 20 m.

The model for $\tilde{c}(t)$ is

$$\tilde{c}(t) \doteq I^s(t) + T^s(t) + E^s(t) - c\delta t^s(t) + M_b^s(t) + \eta_b^s(t) \qquad (6)$$

where $E^s = R(P_b, P^s) - R(P_b, \hat{P}^s)$ is satellite ephemeris error and $c\delta t^s = ct^s - c\hat{t}^s$ is residual satellite clock bias. The goal is for the broadcast data to the rover should allow accurate prediction of the common-mode errors, while being minimally influenced by the noncommon-mode errors at the base. Eqn. (6) shows that $\tilde{c}(t)$ contains both common and noncommon-mode errors; therefore, additional processing is desirable.

The noncommon-mode errors are correlated over only a few minutes whereas common-mode errors are correlated over several hours. Therefore, various forms of low-pass filtering should attenuate the affects of the noncommon-mode errors. Before filtering, it is useful to consider the ionospheric error, which has trends that are predictable using ephemeris data available at each base and rover. When those tends are high, the filtered correction would either lead of lag the present value of $\tilde{c}(t)$. Therefore, the predictable portion of these terms is removed prior to filtering.

Let $\hat{I}^s$ represents the ionosphere delay computed using ephemeris and define

$$\tilde{d}(t) = \tilde{c}(t) - \hat{I}^s \qquad (7)$$

The model for $\tilde{d}(t)$ is

$$\begin{aligned} \tilde{d}(t) &\doteq \delta I^s(t) + T^s(t) + E^s(t) - c\delta t^s(t) \\ &\quad + M_b^s(t) + \eta_b^s(t) \end{aligned} \qquad (8)$$

where $\delta I^s(t) = I^s(t) - \hat{I}^s(t)$. The first line of eqn. (8) contains the desired signal for the corrections. These signals have very small changes in rate over long periods of time (i.e., hours). The second line of eqn. (8) contains the noncommon-mode signals. These signals change rapidly and are zero mean over

several minutes. Therefore, to also attain the ability to predict corrections at future times, the form of low pass filter that we use is line fitting to $\tilde{d}(t)$.

At time $t_0$, the line $a_{t_0} + b_{t_0}(t - t_0)$ is fit to the data

$$\left\{ \tilde{d}(\tau) \text{ for } \tau \in [t_0 - L, t_0] \right\}.$$

The parameters $[a_{t_0}, b_{t_0}, t_0]$ are communicated to the rover arriving at the rover at some time after $t_0$. For any time $t$, the rover computes the correction as

$$\hat{c}(t; t_0) = a_{t_0} + b_{t_0}(t - t_0) + \hat{I}^s(t). \tag{9}$$

Of course, the base and rover must use the same issue of ephemeris data.

For position computations, the rover uses the compensated pseudorange measurement after DGNSS correction:

$$\Delta\rho_r^s(t; t_0) = \rho_r^s(t) - \hat{c}(t; t_0). \tag{10}$$

The correction latency is $l = (t - t_0)$. Assuming perfect cancellation of common-mode errors when $l = 0$, the DGNSS pseudorange model is

$$\begin{aligned} \Delta\rho_r^s(t; t_0) &\doteq R(P_r(t), \hat{P}^s(t)) + (\hat{c}(t; t) - \hat{c}(t; t_0)) \\ &+ M_r^s(t) + \eta_r^s(t). \end{aligned} \tag{11}$$

The term $(\hat{c}(t; t) - \hat{c}(t; t_0))$ accounts for the error in prediction of the common-mode errors due to communication latency.

The dominant error source on the DGNSS compensated pseudorange measurement is the rover multipath $M_r^s$ which can be of several meters in magnitude. Addressing this rover multipath is necessary to achieve meter level performance.

## V. DOPPLER MEASUREMENT INCLUSION

This section discusses the importance of including Doppler measurement to overcome the unobservability issue that is arrived with the inclusion of multipath state in the estimation algorithm.

Suppose, $x \in \mathbb{R}^{n_s}$ denotes the rover state vector, where

$$x(t) = [p^T, v^T, a^T, t_r, d_r, M^s]^T. \tag{12}$$

In eqn. (12) $p, v, a \in \mathbb{R}^3$ represent the rover position, velocity and acceleration, $t_r$ and $d_r$ are the receiver clock bias and drift, $M^s$ multipath error state respectively. Therefore, $n_s = 11 + m$, where $m$ is the number of available satellite measurements. When both pseudorange and Doppler measurements are used, the final observation matrix $H$ becomes

$$H = \begin{bmatrix} \widehat{h}_{m \times 3} & 0_{m \times 3} & 0_{m \times 3} & 1_m & 0_m & I_{m \times m} \\ 0_{m \times 3} & \widehat{h}_{m \times 3} & 0_{m \times 3} & 0_m & 1_m & 0_{m \times m} \end{bmatrix}. \tag{13}$$

When only pseudorange is used, then the second row is dropped. Here, $\widehat{h}_m = [h^1 \ h^2 \dots h^m]^T$ and each $h^s$ is calculated using eqn. (4). Then $I_{q \times q}$ is the identity matrix with $q$ rows and columns and $0_{a \times b}$ is the zero matrix with $a$ rows and $b$ columns. The measurement is unobservable to rover velocity, acceleration and receiver clock drift $v, a$ and $d_r$.

**Example.** The following simplified example is intended to clarify the observability challenges connected to multipath and position estimation. It also clarifies how use of the Doppler measurement enhances the ability to attenuate the effects of multipath on the position estimates.

Consider the following 1-dimensional system with a standard position, velocity and acceleration (PVA) model [36]. The measurement model is in the form of

$$z = Hx + \eta, \tag{14}$$

where the white measurement noise $\eta \sim \mathcal{N}(0, \sigma_\rho^2)$ has $\sigma_\rho = 0.5$ m. The multipath state is modeled as

$$m_p(k+1) = \lambda m_p(k) + \omega_m(k) \tag{15}$$

where $\omega_m \sim \mathcal{N}(0, \sigma_m^2)$. The values of $\lambda$ and $\sigma_m$ are selected so that the correlation time and steady-state covariance $P_m$ of $m_p$ are realistic (i.e., $\lambda = 0.995$, $\sigma_m = 2.87$, and $P_m = 2$). The actual state vectors concatenates the rover state vector with the multipath state such that $x = [p, v, a, m_p]^\top$. The measurement matrix is $H = [1, 0, 0, 1]$.

**Design Scenario 1**: In this sceario, the designer makes the naive decision to design the estimator ignoring the multipath state, defining the estimator state as $\hat{x} = [p, v, a]^\top$ with $H = [1, 0, 0]$, and defining $R = 0.25 = \sigma_\rho^2$. Assuming that the actual state vector is defined to be the same as $\hat{x}$ (i.e., only the PVA states), the designer (optimistically) predicts the steady-state performance as indicate by the blue curve in Fig. 1.[1] When the designer tests the system in the real world (i.e., four states) the observed performance is as indicated by the green curve in Fig. 1.

**Design Scenario 2**: Disappointed with the results of Scenario 1 and realizing the culprit is multipath error, the designer decides to continue with the same three state model, but to increase $R = 4.25 m^2 = \sigma_\rho^2 + \gamma_m^2$, where $\gamma_m = (2m)^2$ is the covariance of the multipath error on the psuedorange. The designer (optimistically) predicts the performance as indicate by the red curve in Fig. 1. When the designer tests the system in the real world (i.e., four states) the observed performance is as indicated by the black curve in Fig. 1. The predicted is better (in the sense of being closer to the actual), but still to conservative. The predicted and actual performance do not match because the design model is assuming that the multipath error is white, while for the actual system the multipath error is correlated in time.

**Design Scenario 3**: This scenario uses the four state model in the design (i.e., including the multipath state). The measurement noise is assumed to be white noise with $R = 0.25 = \sigma_\rho^2$. The system is aware of the fact that there are correlated measurement errors (i.e., multipath) present and optimizes the estimator gain for the scenario.

Because the design and actual models are the same, their performance will match. This performance is shown by the blue curve in Fig. 2. The performance is not as good as that

---

[1]Performance is predicted by (1) computing the steady-state Kalman gain for the design model, (2) using that gain to compute the steady-state covariance of the actual system, (3) extracting the position error standard deviation, and (4) ploting the corresponding folded normal distribution. For additional detail on the analysis approach see Ch. 6 in [9].
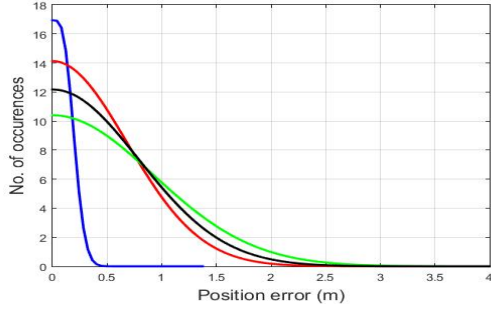
Fig. 1: Position error distribution for scenarios 1 and 2.
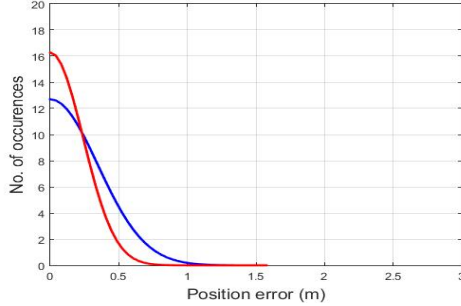


Fig. 2: Position error distribution for scenario 3 and 4

predicted for either of the design models in Fig. 1; however, it makes the correct prediction of the performance and its actual performance is better that either of the actual performances in Fig. 1.

**Design Scenario 4**: The system uses both the pseudorange and Doppler measurements. The measurement vector, $H$ matrix, and measurement covariance matrix are:

$$z = \begin{bmatrix} \Delta\rho_r \\ \lambda D_r \end{bmatrix}, \quad H = \begin{bmatrix} 1 & 0 & 0 & 1 \\ 0 & 1 & 0 & 0 \end{bmatrix}, \quad R = \begin{bmatrix} \sigma_\rho^2 & 0 \\ 0 & \sigma_d^2 \end{bmatrix}$$

with $\sigma_d = 0.04$ m.

This performance is shown by the red curve in Fig. 2. The performance is better than that predicted for Scenario 3. This result should be obvious, as more information has been used to generate the estimate in Scenario 4, the specific contribution of the information is interesting. In Scenario 3, while the state is observable, the position and multipath are not highly separable. Adding the Doppler measurement in Scenario 4 directly measures the velocity, which greatly enhances the ability of the state estimator to seperably estimate $p$ and $m_p$. The condition number of the observability matrix for Scenario 3 is more that 50000 times that of Scenario 4.

## VI. Experimental Results

This section considers experimental data studying position performance relative to the one-meter accuracy specification and sensitivity to latency effects.

### A. Experimental Data Description

The GNSS receiver was consumer-grade and single-frequency (u-blox M8T). All results are produced using only pseudorange and Doppler. No phase measurements were considered.

The DGNSS correction data were obtained using the RTCM standard [10] and NTRIP protocol from two base stations: ESRI (baseline separation 14.5 km) and UCR (baseline separation 6 m). The DGNSS correction parameters $[a_{t_0}, b_{t_0}, t_0]$ are computed and stored in rover (using $L = 500$). This value of $L$ was selected to be about four times the expected base multipath correlation time. For the subsequent results, data is post-processed and delayed DGNSS correction parameters are used to study the effects of latency.

All the results shown in this section are conducted for a stationary rover with the GNSS receiver connected to an antenna at a surveyed location. The stationary rover state estimation algorithm has parameters tuned for a rover that is in motion (not stationary). The intent is to study the performance that would be achieved by an aided inertial system, where the inertial system is designed to remove the mean motion of the rover.

### B. Position Estimation Algorithms

This section reports positioning accuracy experimental results for 3 different incremental algorithms:

1) an 11 state Kalman Filter (KF) with state defined as $x(t) = [p^T, v^T, a^T, t_r, d_r]^T$ using only pseudorange measurements;
2) an $(11+m)$ state KF with the state defined in eqn. (12) using only pseudorange measurements; and,
3) an 11 + multipath state KF with the state defined in eqn. (12) with pseudorange and Doppler measurements.

All the Kalman filter implementations use a PVA model [36]. Each algorithm is used to process the entire batch of measurements ($k = 1, \ldots, 1600$ seconds) to estimate the trajectory for a given value of the latency $l$, using correction $\hat{c}(k; k - l)$ from eqn. (9). For algorithm $n$ and latency $l$, this produces the state sequence $P_{k,l}^n$. The experiment is repeated for each algorithm for latency values $l = 0, \ldots, 1200$ seconds.

For algorithm $n$, time epoch $k$, and correction latency $l$, the norm of horizontal position error is

$$e_{h_{k,l}}^n = \|P_r - P_{k,l}^n\| \tag{16}$$

where $P_r$ is the known antenna position.

### C. Positioning Accuracy

Fig. 3(a-c) show histograms of the distribution norm of horizontal position error $e_{h_{k,l}}^n$ defined in eqn.16 for latency $l = 0$. The red curve depicts the best fit of a Rayleigh distribution. Each graph is for a different algorithm as summarized in Section VI-B.

Table I summarizes various measures of positioning accuracy when the latency is zero. Column 1 shows the algorithm number $n$. Column 2 shows the mean horizontal position error defined in eqn. 16. Column 3 contains the standard deviation horizontal position error. Column 4 reports percentage of the samples that have a horizontal positioning error less than one
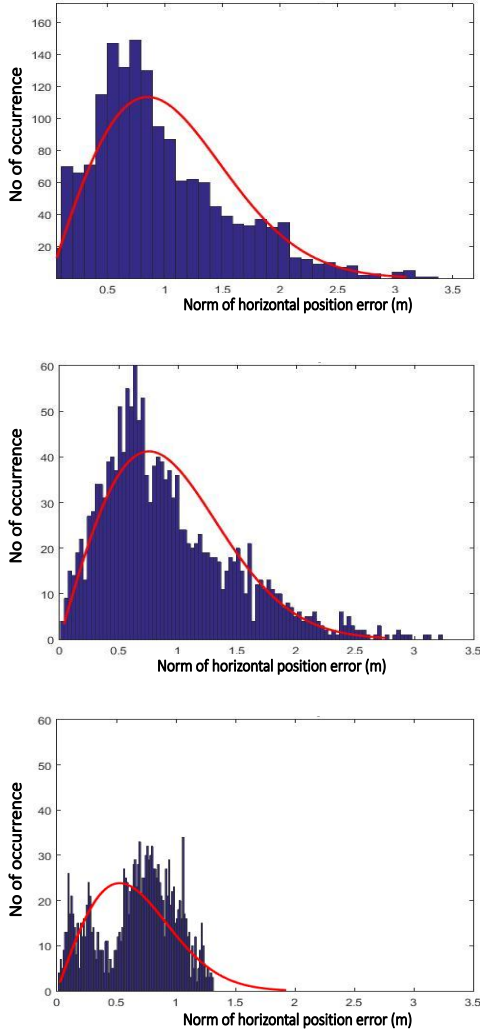
Fig. 3: (Top) Distribution plot for Algorithm 1, (Middle) Algorithm
(Bottom) Algorithm 3.

TABLE I: Positioning Performance

| Algorithm | Mean $e_h$ (m) | Std. Dev. $e_h$ (m) | Probability $e_h < 1$ m (%) | Max. $e_h$ (m) |
|---|---|---|---|---|
| 1 | 0.97 | 0.7 | 63 | 3.3 |
| 2 | 0.91 | 0.56 | 65 | 3.4 |
| 3 | 0.67 | 0.32 | 85 | 1.3 |

meter. Column 5 reports the maximum value of the horizontal
position error.

Fig. 3 and Table I demonstrate that adding the multipath
states and the Doppler measurement each improve the perfor-
mance.

### D. Correction Sensitivity to Latency

The correction error due to communication latency is

$$e_c(k,l) = |\hat{c}(k;k) - \hat{c}(k;k-l)|,$$

where $\hat{c}(k;k)$ is the correction with no latency and $\hat{c}(k;k-l)$
is the correction with latency $l$ both calculated using eqn. (9).
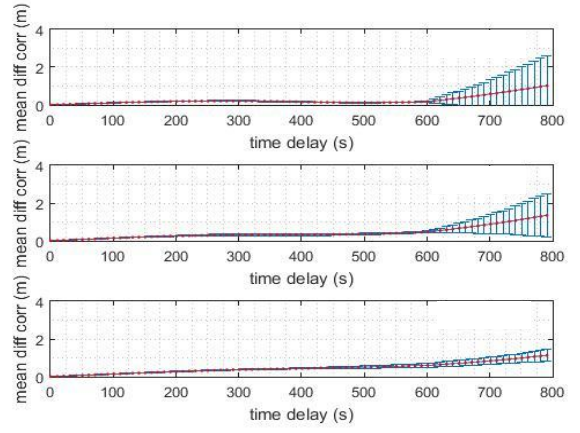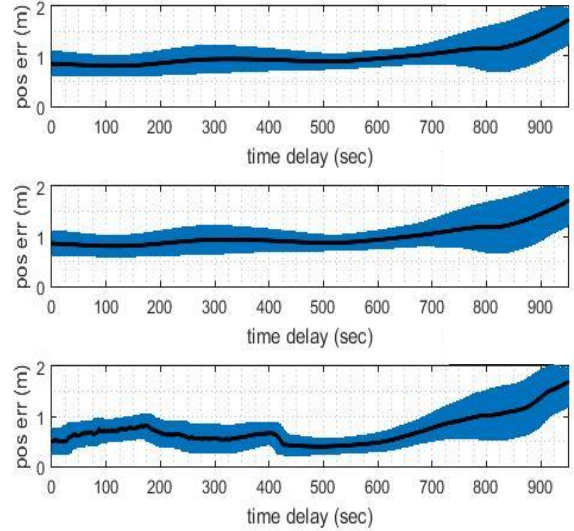


Fig. 4: Correction difference vs latency



Fig. 5: Position error vs latency. (Top) Algorithm 1. (Middle) Algorithm 2.
(Bottom) Algorithm 3.

For each fixed value of $l$, the mean and standard deviation of
$e_c(k,l)$ are computed from the experimental data. Fig. 4 shows
the mean plus and minus the standard deviation of $e_c(k,l)$ as
a function of $l$ for three satellites. The graphs remain less than
one meter for up to 600 seconds.

### E. Positioning Sensitivity to Latency

For each of the three algorithms described in Section VI-B,
Fig. 5 illustrates the effect of the DGNSS correction latency
$l$ on GNSS position accuracy as measured by $e_{h_{k,l}}^n$ defined
in eqn. (16). In each graph, the black curve shows the mean
of $e_{h_{k,l}}^n$. Each point on the graph is also marked with a one-
standard-deviation error bar.

Fig. 5 shows that position estimation accuracy is insensitive
to communication latency for delays up to 600S.

## VII. Conclusion and Future Work

Real-time positioning relative to the ECEF frame is one of the primary requirement of navigation technology in important commercial applications - connected vehicle, autonomous navigation. Data communication latency and interruptions are the real-life challenges that all real-time systems encounter and are the main focus of this research project. Reliably achieving sub-meter positioning accuracy using inexpensive consumer-grade sensors was another motivation of this research project.

This paper discussed GNSS measurement error characteristics relative to the challenge of maintaining meter-level ECEF position estimates in the presence of correction communication latency. The paper provides an algorithm to compensate both latency and lost DGNSS correction messages. The prime contributions of this paper are: (1) demonstrating that positioning performance insensitive to correction latency up to 600 s; and (2) demonstating horizontal position estimation accuracy at the submeter level 85% of the samples.[2],

This paper also discussed how different algorithmic and multipath modeling choices affect the achievable position accuracy.

Future research will focus on extending the results herein to vehicle positioning performance on maneuvering platforms in real-time, including the use of inertial navigation.

## VIII. acknowledgement

## References

[1] P. Misra and P. Enge, "Special issue on global positioning system," *Proc. of the IEEE*, vol. 87, no. 1, pp. 3–15, 1999.

[2] B. Hofmann-Wellenhof, H. Lichtenegger, and J. Collins, *"Global Positioning System: Theory and Practice"*. Springer Science & Business Media, 2012.

[3] G. Blewitt, "Basics of the GPS Technique: Observation Equations," *Geodetic applications of GNSS*, pp. 10–54, 1997.

[4] C. Shuxin, Y. Wang, and C. Fei, "A study of differential GNSS positioning accuracy," *in 3rd Int. Conf. on Microwave and Millimeter Wave Tech.*, pp. 361–364, 2002.

[5] S. Johnson, L. Rolfes *et al.*, "Connected Vehicle Pilot Deployment Program Phase II Data Privacy Plan-Tampa (THEA)." Tech. Rep., February, 2017. [Online]. Available: https://www.its.dot.gov/pilots/index.htm

[6] S. Cadzow *et al.*, "Connected Vehicle Pilot Deployment Program Phase 2: Data Privacy Plan-New York City."," Tech. Rep., December, 2016. [Online]. Available: https://www.its.dot.gov/pilots/index.htm

[7] F. M. Kitchener, T. English *et al.*, "Connected Vehicle Pilot Deployment Program Phase 2, Data Management Plan-Wyoming." Tech. Rep., April, 2017. [Online]. Available: https://www.its.dot.gov/pilots/index.htm

[8] P. Teunissen and O. Montenbruck, "Springer Handbook of Global Navigation Satellite Systems," vol. 26(2), p. 762, 2017.

[9] J. A. Farrell, *"Aided Navigation: GNSS with High Rate Sensors"*. McGraw-Hill Inc, 2008.

[10] Anonymous, "RTCM Standard 10403.2 for Differential GNSS (Global Navigation Satellite Systems) Services," RTCM Special Committee, Tech. Rep., August, 2001.

[11] P. K. Enge, R. M. Kalafus, and M. F. Ruane, "Differential operation of the global positioning system," *IEEE Comm. Mag.*, vol. 26(7), pp. 48–60, 1988.

[12] P. Teunissen, "Differential GPS: Concepts and Quality Control," *Netherlands Institution of Navigation, Amsterdam*, 1991.

[13] J. A. Farrell, M. Grewal, M. Djodot, and M.Barth, "Differential GNSS with latency compensation for autonomous navigation," *Int. Symp. on Int. Cont.*, pp. 20–24, 1996.

[14] J. A. Farrell, M. Djodat, M. Barth, and M. Grewal, "Latency compensation for differential GPS," *Navigation*, vol. 44(1), pp. 99–107, 1997.

[15] M. S. Braasch and A. Van Dierendonck, "GPS receiver architectures and measurements," *Proc. of the IEEE*, vol. 87(1), pp. 48–64, 1999.

[16] M. S. Grewal, L. R. Weill, and A. P. Andrews, *"Global Positioning System, Inertial Navigation,and Integration"*. John Wiley & Sons, 2007.

[17] P. Misra and P. Enge, "Global Positioning System: Signals, Measurements and Performance, second edition," *Massachusetts: Ganga-Jamuna Press*, 2006.

[18] B. W. Parkinson, J. Spilker, and P. Enge, "Global Positioning System: Theory and Applications," *AIAA*, vol. 2, pp. 3–50, 1996.

[19] P. Enge, "The global positioning system: Signals, measurements, and performance," *Int. J. of Wireless Info. Net.*, vol. 1(2), pp. 83–105, 1994.

[20] G. Wübbena, A. Bagge, G. Seeber, V. Böder, P. Hankemeier *et al.*, "Reducing distance dependent errors for real-time precise DGPS applications by establishing reference station networks," *Proc. OF ION GPS*, vol. 9, pp. 1845–1852, 1996.

[21] C. Kee, B. W. Parkinson, and P. Axelrad, "Wide area differential GPS," *Navigation*, vol. 38(2), pp. 123–145, 1991.

[22] P. Enge, T. Walter, S. Pullen, C. Kee, Y.-C. Chao, and Y.-J. Tsai, "Wide area augmentation of the global positioning system," *Proc. of the IEEE*, vol. 84(8), pp. 1063–1088, 1996.

[23] L. Dai, S. Han, J. Wang, and C. Rizos, "A study on GPS/GLONASS multiple reference station techniques for precise real-time carrier phase-based positioning," *Proc. of ION GPS*, pp. 392–403, 2001.

[24] P. Loomis, G. Kremer, and J. Reynolds, "Correction algorithms for differential GPS reference stations," *Navigation*, vol. 36(2), pp. 179–193, 1989.

[25] G. T. Kremer, R. M. Kalafus, P. V. Loomis, and J. C. Reynolds, "The effect of selective availability on differential GPS corrections," *Navigation*, vol. 37, no. 1, pp. 39–52, 1990.

[26] Y. Saber, R. Antri-Bouzar, M. Sebeloue, and J. Boucher, "Comparison between two navigation modes for differential GPS," *Proc. of IEEE Microwave and Millimeter Wave Tech. Conf.*, pp. 463–466, 1998.

[27] B. Park, J. Kim, and C. Kee, "RRC unnecessary for DGPS messages," *IEEE T. on Aero. and Elec. Sys.*, vol. 42(3), 2006.

[28] B. Townsend and P. Fenton, "A practical approach to the reduction of pseudorange multipath errors in a L1 GPS receiver," *Proc. of the 7th Int. Tech. Meeting of the Sat. Div. of the ION*, 1994.

[29] F. Lee, S. Chun, Y. J. Lee, T. Kang, G. Jee, and J. Kim, "Parameter estimation for multipath error in GPS dual frequency carrier phase measurements using unscented Kalman filters," *Int. J. of Cont., Auto., and Sys.*, vol. 5(4), pp. 388–396, 2007.

[30] J. K. Ray, *"Mitigation of GPS Code and Carrier Phase Multipath Effects Using a Multi-Antenna System"*. University of Calgary, 2000.

[31] J. M. Tranquilla, J. Carr, and H. M. Al-Rizzo, "Analysis of a choke ring groundplane for multipath control in global positioning system (GPS) applications," *IEEE T. on Ant. and Prop.*, vol. 42(7), pp. 905–911, 1994.

[32] L. Serrano, D. Kim, R. B. Langley, K. Itani, and M. Ueno, "A GPS velocity sensor: how accurate can it be?–a first look," *ION NTM*, vol. 2004, pp. 875–885, 2004.

[33] L. Serrano, D. Kim, and R. B. Langley, "A single GPS receiver as a real-time, accurate velocity and acceleration sensor," *Proc. of the 17th Int. Tech. Meeting of the Sat. Div. of ION*, vol. 2124, 2004.

[34] M. D. Agostino, A. Manzino, and G. Marucco, "Doppler measurement integration for kinematic real-time GPS positioning," *Applied Geomatics*, vol. 2(4), pp. 155–162, 2010.

[35] J. An and J. Lee, "Improvement of GPS position estimation using SNR and Doppler," *in IEEE Int. Conf. on AIM*, pp. 1645–1650, 2017.

[36] R. Brown and P. Hwang, *"Introduction to Random Signals and Applied Kalman Filtering"*. Wiley, New York, 1996.

[37] E. Aghapour, F. Rahman, and J. A. Farrell, "Risk-averse performance-specified state estimation," *Proc. of IEEE/ION PLANS, in press*, 2018.

[2]A companion paper at this conference [37] presents a new estimation algorithm achieving submeter horizontal accuracy in excess of 90% of the samples.